detritus | Multidisciplinary Journal for Circular Economy and Sustainable Management of Residues

CISA

EFFECT OF BOUNDARY CONDITIONS ON THE METHANE OXIDATION EFFICIENCY IN LANDFILL PILOT-SCALE BIOFILTERS

Jeovana Jisla das Neves Santos [1], Mauro Duarte de Oliveira Neto [1], Yohan Dulac [1], Jordan Carneiro Martins de Souza [1], Federico Galli [2,*] and Alexandre Cabral [1]

[1] *Department of Civil and Building Engineering, University of Sherbrooke, Quebec, Canada*
[2] *Department of Chemical and Biotechnological Engineering, University of Sherbrooke, Quebec, Canada*

Article Info:
Received:
19 December 2025
Revised:
27 March 2026
Accepted:
8 April 2026
Available online:
27 April 2026

Keywords:
Biofilter performance
Landfill gas
Methane loading
Boundary conditions
Methane biofiltration
Oxidation efficiency

ABSTRACT

This study compares the performance of two pilot-scale biofilters designed to mitigate methane emissions at the Complexe Environnemental de Saint-Michel (CESM) landfill in Montreal, Canada. Although both systems shared the same geometry, they differed in materials and boundary conditions. CESM1 used a compost-woodchip mixture, while CESM2 incorporated a compost-gravel blend (STEM) and was partially enclosed to enable continuous monitoring. Field measurements showed that CESM1 consistently achieved higher methane oxidation efficiency and greater temporal stability. In contrast, CESM2 exhibited performance variability, particularly during the summer 2024, when internal heating and surface cracking were observed under the shelter enclosure. These conditions may have affected gas distribution and methanotrophic activity. Batch tests confirmed reduced microbial oxidation capacity in CESM2, prompting corrective interventions such as surface tilling and zone-specific repairs. Despite lower efficiency, CESM2 oxidized a higher total mass of methane due to substantially greater loading rates. Both systems followed seasonal trends, suggesting ambient temperature as a contributing factor. The results underscore the importance of adapting biofilter design to site-specific boundary conditions, especially in enclosed configurations where thermal and moisture dynamics may deviate from open-field scenarios. While engineered media such as STEM can support methane oxidation, their performance is contingent on appropriate structural and environmental management. From a design perspective, ensuring adequate gas distribution, preventing excessive heat accumulation, and maintaining moisture balance are critical to sustaining methane oxidation performance. In enclosed systems, additional attention should be given to surface integrity to avoid preferential pathways and reduced performance.

1. INTRODUCTION

Anaerobic degradation of organic matter in landfills generates biogas, primarily composed of methane (CH_4) and carbon dioxide (CO_2). Landfills contribute approximately 630 Mt CO_2-equivalent globally (Gebert et al., 2022), with methane (CH_4) emissions from the waste sector accounting for 28% of total Canadian methane emissions in 2022 (ECCC, 2022). Although methane is short-lived (12-14 years), it has a global warming potential 81-86 times greater than CO_2 over a 20-year horizon. This makes it a strategic target for short-term climate change mitigation.

Methane oxidation biosystems (MOBs) offer a low-cost strategy for reducing CH_4 emissions, especially when gas production is too diluted (less than 20-30% v/v), or too low (typically below 15-30 m³/h) to allow energy recovery or flaring (Farrokhzadeh et al., 2017; Huber-Humer et al., 2008). The Intergovernmental Panel on Climate Change (IPCC) has recognized MOBs as a promising option for the waste sector (Gebert et al., 2022).

MOBs can be grouped into three categories: biocovers (integrated into the landfill cover layer), biowindows (localized oxidation zones targeting emission hotspots), and biofilters (standalone engineered systems treating collected landfill gas). They differ based on their integration with site operating conditions and their functional design. These biosystems rely on a multilayer structure where the gas distribution layer (GDL) feeds landfill gas into the methane oxidation layer (MOL), rich in organic matter and supporting methanotrophic bacteria (Duan et al., 2022).

Recent efforts have focused on optimizing biofilter design (Ahoughalandari et al., 2018; Scheutz et al., 2023), but

* Corresponding author:
Federico Galli
email: federico.galli@usherbrooke.ca

https://doi.org/10.31025/2611-4135/2026.19588

technical challenges remain. A common limitation is pore occlusion and clogging of the MOL, due to extracellular polymeric substances (EPS) produced by methanotrophs, which reduce gas diffusivity (He et al., 2017). Hydraulic performance is equally critical. Poorly selected MOL materials may cause capillary barrier effects at the GDL/MOL interface. This can lead to localized hydraulic blockages, methane overload in specific areas, and lateral gas bypass along preferential pathways (Gebert et al., 2022).

To mitigate these effects, Structured Engineered Medium (STEM), composed of compost and structuring agents (e.g., woodchips, gravel), have been proposed. These media combine microbial support and air-filled porosity, improving gas diffusion, water drainage, and moisture control (Dulac et al., 2024; Dulac & Cabral, 2025; Gebert et al., 2022).

Beyond material choice, construction parameters, such as slope, geometry, and layering, also influence performance. Dulac et al. (2024) confirmed the potential of numerical models to predict hydraulic behavior and support simplified design. This approach relies on representative geotechnical and climatic data, along with well-defined boundary conditions. The authors also highlight the value of instrumented field-scale MOBs to better calibrate pre-design simulations.

This study draws on data from two biofilters built during different phases of a research project at the CESM site in Montreal, Canada. Although constructed at different times with varying materials and operational strategies, both systems shared the same geometry and location. This study aims to contrast the methane oxidation performance of two biofilters under varying boundary conditions and identify the key operational and design features influencing MOL's effectiveness. The analysis focuses on integrated system performance rather than isolating individual parameters. This is particularly relevant due to the presence of a shelter enclosure in one system, which was associated with a separate continuous monitoring study beyond the scope of this work. This study advances existing research by providing a controlled, field-scale comparison of two pilot biofilters sharing identical geometry and siting but differing in methane oxidation layer composition and boundary conditions (open versus partially enclosed). Unlike earlier studies that focused primarily on material optimization or modeling-based design, this work explicitly isolates the influence of enclosure-induced thermal and hydric constraints on biofilter performance. The results offer new, practical evidence on how boundary conditions can override intrinsic material properties and fundamentally alter methane oxidation efficiency at field scale.

2. MATERIALS AND METHODS

2.1 Description of study area

The Complexe Environnemental de Saint-Michel (CESM) is a former 72-hectare landfill site located in Montreal, now in its after-care phase. Developed within a former limestone quarry reaching depths of up to 80 meters, the site received approximately 40 million tons of waste between 1968 and 2008 (Lagos et al., 2017). As part of the City of Montreal's climate commitments (Climate Plan 2020-2030), which targets carbon neutrality by 2050 (City of Montréal, 2020), mitigating methane emissions at CESM has become a key priority (Almeida et al., 2024), making it an ideal site for field-scale validation of methane oxidation technologies.

Landfill gas (LFG) at the site is collected from two sources: (1) a network of gas wells used for electricity generation, and (2) a collection system installed in ventilation trenches. The latter, while associated with high flow rates, contains very low methane concentrations (typically below 2% by volume), mainly due to the strong vacuum applied by the blower system to prevent odor dispersion toward nearby residential areas. Given its low energy potential, this lean LFG could not be treated using conventional methods. It was therefore targeted in a research project focused on developing large-scale biofiltration as a mitigation strategy. Pilot-scale biofilters were designed, constructed, and instrumented on site to experimentally treat approximately one-tenth of the total gas flow (Almeida et al., 2024; Franzidis et al., 2008).

2.2 Selection of materials

The present study covers two phases of analysis involving biofilters installed at the CESM site, allowing direct comparison under site-specific conditions and progressive design refinement: CESM1, conducted from 2021 to 2022, and CESM2, ongoing since 2023.

For CESM1, a 1:1 volumetric blend of compost and wood chips, sourced from the CESM's on-site composting platform for leaves and branches, was selected based on its demonstrated methane oxidation capacity, field workability, and geotechnical performance. This mixture met the minimum efficiency threshold of 70% required by the City of Montreal (Almeida et al., 2024).

2.2.1 Design lessons from CESM biofilter – Phase 1

A key lesson from CESM1 was that the fine sand layer (used as a filter layer between the MOL and the GDL) caused clogging due to compost migration and cementation, highlighting the importance of layer compatibility. We hypothesize that high temperatures during the acclimatization phase accelerated wood chip degradation into fine compost, which migrated into the sand layer. Subsequent water infiltration may have promoted cementation, leading to significant clogging at the MOL interface along a substantial portion of the biofilter.

To prevent similar clogging phenomena observed in CESM1, the sand-based filter layer was eliminated in the CESM2 configuration. Additionally, MOL was reengineered using a 1:1 volumetric blend of compost and gravel mixture, favoring gravel as a structuring agent over wood chips. This approach aimed to enhance air-filled porosity and promote more uniform gas distribution within the biofilter.

2.3 MOL Material Properties

Table 1 summarizes the geotechnical and methane oxidation properties of the MOL materials employed in the CESM1 and CESM2 biofilters.

The compost-woodchips mixture (CESM1) had higher sand content and total porosity, due to the structural role of wood chips as bulking agents promoting aeration. In contrast, the compost-gravel mixture (CESM2) showed lower porosity and a predominance of coarse particles, which may offer hydraulic benefits by reducing saturation risks and limiting capillary barrier effects at the GDL/MOL interface.

A notable difference in organic matter content is observed between the two phases.

The choice of MOL material for CESM2 was guided by the work of La et al., 2018, who recommend an effective compost proportion of 12.5-25%, corresponding to a target organic matter content (measured by standard loss-on-ignition method) of 5-10% in the final mixture. For compost containing 25.1% organic matter, this translates to a recommended compost proportion of approximately 20-40% (i.e., 5-10%÷25.1%). The selected 1:1 volumetric ratio (50% compost and 50% gravel) therefore slightly exceeds this range, ensuring sufficient nutrient availability.

Column test results (not covered in this study) showed a maximum methane oxidation rate ($V_{máx}$) of 2,383 $g \cdot m^{-3} \cdot day^{-1}$ for CESM1 STEM, approximately 32% higher than the value observed for CESM2 (1624 $g \cdot m^{-3} \cdot day^{-1}$). This enhanced performance appears to be associated with the physical properties of the material, particularly its higher organic matter content, which may improve moisture retention and increase the available surface area for microbial colonization. In addition, greater nutrient availability in the compost substrate may have further supported methanotrophic activity.

Moreover, the K_m value for CESM1 was significantly lower (12 $g \cdot m^{-3}$) compared to CESM2 (23.4 $g \cdot m^{-3}$). The parameter K_m represents the half-saturation constant from Michaelis–Menten kinetics, corresponding to the methane concentration at which the oxidation rate reaches half of its maximum value (V_{max}). Lower K_m values indicate a higher affinity of methanotrophic microorganisms for CH_4, reflecting greater oxidation efficiency at low CH_4 concentrations. However, these differences should be interpreted within the broader context of design priorities and operational conditions. While CESM1 favored microbial activity due to its more active and porous structure, CESM2 incorporated gravel, a material chosen for its structural stability and drainage performance, in line with established design recommendations.

2.4 Construction

2.4.1 CESM Biofilter – phase 1

The biofilter studied herein was built with a rectangular footprint of 50 m² (5 m × 10 m) and a total height of approximately 1.45 m. Its structure consisted of stacked concrete blocks forming vertical walls, sealed with urethane, and lined internally with an HDPE geomembrane. A geotextile layer was placed over the base to protect the geomembrane. The GDL, 0.30 m thick, consisted of two types of gravel (¾" and ¼"), overlaid by a 0.10 m sand filter layer. As previously described, the MOL was composed of a 1:1 volumetric mix of leaf compost and woodchips, with an approximate thickness of 1 m. To maintain positive temperatures within the biofilter during winter, a heat trace system was laid between the sand and MOL layers, ensuring suitable conditions for methanotrophic activity.

Water content and temperature probes were installed at different depths within the biofilter, including near the surface (0.05 m and 0.10 m) and close to the interface between MOL and GDL (0.90 m and 0.95 m), to monitor potential capillary barrier effects. Most of the sensors were allocated to Zones 1 and 2, where greater spatial variability was expected. The detailed configuration and instrumentation of CESM1 have been previously described by Almeida et al. (2024).

Prior to full-scale operation, an acclimatization phase was conducted in early July 2021 using an external setup. The apparatus consisted of a geotextile base covered with a first layer of compost, followed by the installation of a fishbone-type biogas distribution system, and a second compost layer on top, forming a sandwich-like structure. This setup was supplied with biogas containing approximately 40% CH_4. Injection was maintained at 0.05 CFM (2.03 $m^3.day^{-1}$) for the first two weeks and increased to 0.1 CFM (4.08 $m^3.day^{-1}$) during the third week (Almeida et al., 2024).

Once filled, the biofilter was connected to the main biogas supply system, with an average flow rate of 1 944 $m^3.day^{-1}$ (48 scfm) provided by a blower. Due to operational constraints, methane concentration at the inlet varied significantly, ranging from 0.1% to 4.6%. As a result, the biofilter operated under a transient methane loading regime.

The CESM1 phase concluded with the end of performance monitoring in November 2022. In the summer of 2023, the materials constituting the MOL and the GDL were removed in preparation for the implementation of the next phase.

2.4.2 CESM Biofilter – phase 2

By retaining the same wall structure as in the first phase, CESM2 preserved the geometry of the original biofilter while implementing a new construction plan. The GDL was reinstalled using the same gravel size fractions (¾" and ¼"), as it had been damaged during the removal of the sand filter layer. Once the concrete block walls were re-exposed, they were covered with a geotextile and sprayed with a polyurea membrane to ensure sealing equivalent to the HDPE geomembrane used previously.

Multiple sensors were installed in CESM2 to monitor water content and temperature at different depths (0.10 m, 0.35 m, 0.50 m, 0.75 m, see Supplementary Material I). The water content was monitored using 5TM sensors (Decagon Devices, USA), while temperature was measured using DRF sensors. However, due to operational issues, data acquisition was only possible from October 2024 onward (see Suplemmentary material), as the data logging system was partially damaged during the summer of 2024.

Despite this limitation, water content and temperature profiles were obtained for October 2024, along with average temperature data for the October-December period

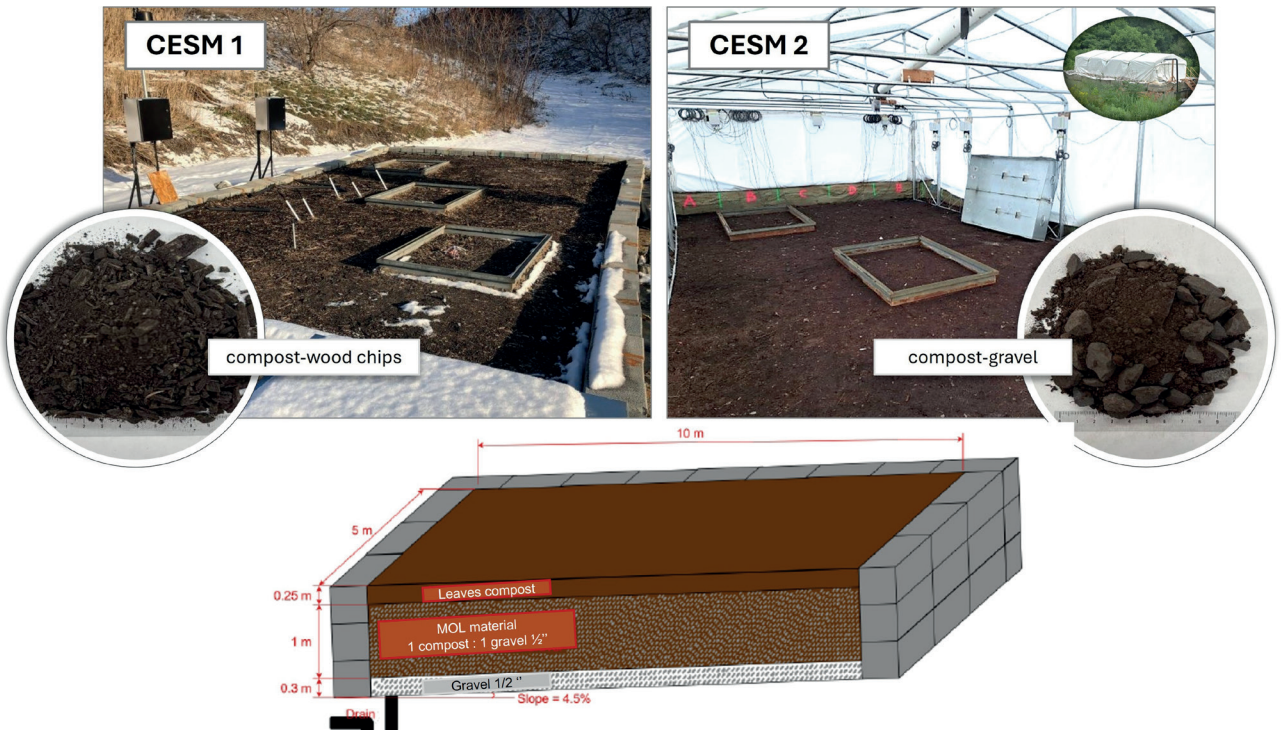

FIGURE 1: Side-by-side comparison of the CESM1 and CESM2 biofilters, showing changes in MOL structure and cross-section scheme of the biofilter.

and temperature measurements at the interface MOL/GDL, at approximately 1 m depth.

The MOL was filled in the fall of 2023. The principle of using a STEM was retained, maintaining the 1:1 volumetric ratio between compost and structural support. However, the composition was modified by replacing the woodchips used in CESM1 with gravel ½" (Figure 1).

The main distinction of CESM2 lies in its objective to enable continuous monitoring of CH_4 oxidation efficiency through a more reliable measurement approach, which, in this project, is used to support and validate the point-in-time measurements obtained with flux chambers. To achieve this, the entire biofilter was enclosed within a partially sealed shelter functioning as a full-scale flux chamber. Details of the continuous monitoring system are part of a separate publication (Souza et al. 2025).

As in CESM1, the CESM2 biofilter operated under a transient methane loading regime. Biogas injection relied on the same supply system, with inlet methane concentrations exhibiting broader variability and generally higher values, ranging from 0.1% to 9.3%. To accommodate these fluctuations, the injection flow rate was manually adjusted, as required by operational conditions, between 815 and 1200 m^3 day^{-1} (approximately 20 to 30 scfm).

2.5 Monitoring

2.5.1 Methane load

For both phases, the biogas flow entering the biofilter was measured using a thermal mass flow meter installed directly at the inlet, upstream of the fishbone-type gas distribution system. The methane loading ($gCH_4.m^{-2}.day^{-1}$) was calculated using Equation 1.

$$Load_{CH_4} = Q \times 1000 \times \left(\frac{16.04}{22.4} \times \frac{1}{S}\right) \times \frac{C_{CH_4}}{100} \times \left(\frac{273}{273 + T_{ext}}\right) \times \times \frac{Patm}{1013} \quad (1)$$

Where Q is the biogas flow rate ($m^3.day^{-1}$), S is the biofilter surface area (m^2), C_{CH4} is the inlet methane concentration (%) measured using a portable gas analyzer (SEM5000, QED Environmental Systems Inc., 2017) with laser technology to measure CH_4 from 0.5 ppm to 100 % (vol), T_{ext} is the ambient temperature (°C), and P_{atm} is the atmospheric pressure (hPa). Figure 2 presents a comparative analysis of daily methane loadings applied to the CESM1 and CESM2 biofilters using violin plots. Figure 2 shows that methane loading values are broadly distributed for both systems, with similar median values (≈309 $g{\cdot}m^{-2}{\cdot}day^{-1}$ for CESM1 and ≈303 $g{\cdot}m^{-2}{\cdot}day^{-1}$ for CESM2), but with substantial variability and a wide range of loading conditions observed in both cases.

2.5.2 Methane outlet flux

Methane surface fluxes at the biofilter were estimated using a static flux chamber. The method involves placing the chamber directly on the surface and monitoring the increase in methane concentration over a fixed time interval (10 minutes in the context of this study). Assuming a linear concentration rise, the slope of the best-fit line (dC/dt) represents the accumulation rate of methane inside the chamber. This volumetric concentration change was then converted into a mass flux using the ideal gas law (Abichou et al., 2006). Equation 2 was used to calculate the surface flux, considering the dimensions of the rectangular chamber used in this project.

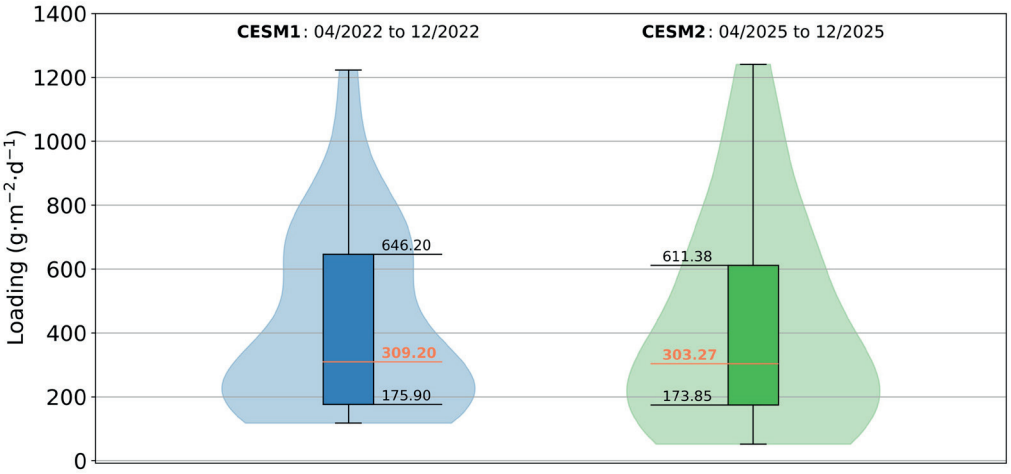

FIGURE 2: Distribution of methane loadings applied to the CESM1 and CESM2 biofilters, shown as violin plots. Both systems exhibit similar median loadings, but CESM2 shows a wider distribution and more frequent high-loading events, reflecting greater operational variability.

$$Flux_{CH_4}\left(\frac{g}{m^2.day}\right) = Slope_{ppm\,x\,s} \times \left[\left(\frac{16.04}{22.4}\right) \times \left(\frac{273}{273 + T_{ext}}\right) \times \right.$$
$$\left. \times \left(\frac{Patm}{1013}\right)\right] \times \left(\frac{V}{S}\right) \times 86.4 \qquad (2)$$

Where corresponds to the rate of change in methane concentration over time (based on the linear fit between two measurements), T_{ext} is the ambient temperature (°C), P_{atm} is the atmospheric pressure (hPa), V and S represent the volume (m³) and surface area (m²) of the flux chamber, respectively.

For this project, the biofilter was divided into three distinct zones, all of which were tested using the flux chamber during the measurement campaigns. This approach aimed to provide a more representative assessment of the overall surface flux, by allowing the results to be weighted according to zone.

2.5.3 Methane oxidation efficiency

Methane oxidation efficiency was estimated under the following assumptions: (i) uniform distribution of inlet gas across Zones 1-3, (ii) negligible methane storage within the system (steady-state conditions), and (iii) no correction for CO_2 production or O_2 consumption. Surface flux measurements are assumed to be representative of average zone-scale emissions.

These assumptions are suitable for integrated field-scale comparison but may bias estimates for CESM2. As surface cracking and preferential pathways developed (Section 3.1), the assumption of uniform gas distribution was likely violated, potentially leading to apparent under- or over-estimation of oxidation efficiency at the system scale rather than reflecting intrinsic MOL performance.

Methane oxidation efficiency was determined using a mass balance approach, based on inlet and outlet CH_4 fluxes, following the methodology described in Almeida et al. (2024). This approach provides an integrated assessment of system performance under field conditions and is widely used in biosystems studies. However, CO_2 production and O_2 consumption were not measured in this study. While multi-gas monitoring could offer additional insights into the biological mechanisms involved in methane oxidation, the adopted method allows for a robust evaluation of overall CH_4 removal efficiency. As previously mentioned, flux chamber measurements were conducted in three distinct zones (Figure 3 provides a schematic overview of these zones).

For the analysis presented in this paper, we assumed that the biogas entering the GDL is evenly distributed across the entire GDL/MOL interface, implying that the different zones exert an equivalent influence on methane oxidation. We adopted this simplifying assumption to facilitate the analysis, but we will re-evaluate it in future publications. In practice, however, biofilters may exhibit non-uniform gas distribution due to physical processes such as capillary barrier effects and partial clogging. These mechanisms can reduce gas permeability in the downslope region (Zone 1), promoting preferential gas migration toward other zones, consistent with the behavior described by Almeida et al. (2024) in Scenario C.

Gas concentration profiles were not monitored in this study due to technical limitations associated with gas sampling probes. Specifically, clogging issues in several probes installed in CESM1 (Almeida et al. 2024), which compromised the reliability of the measurements. Therefore, to ensure consistency between systems, gas profiles were not included for CESM2.

2.6 Statistical analysis

Descriptive statistical analyses were performed to characterize the datasets from CESM1 and CESM2, including calculation of mean, median, minimum, maximum, and standard deviation for the main performance parameters. Data normality was evaluated using the Shapiro-Wilk test to assess whether the variables conformed to a normal distribution.

As the majority of the datasets did not satisfy the assumption of normality ($p < 0.05$), non-parametric Mann–Whitney U tests were applied to compare methane loading, oxidation efficiency, and the amount of methane oxidized

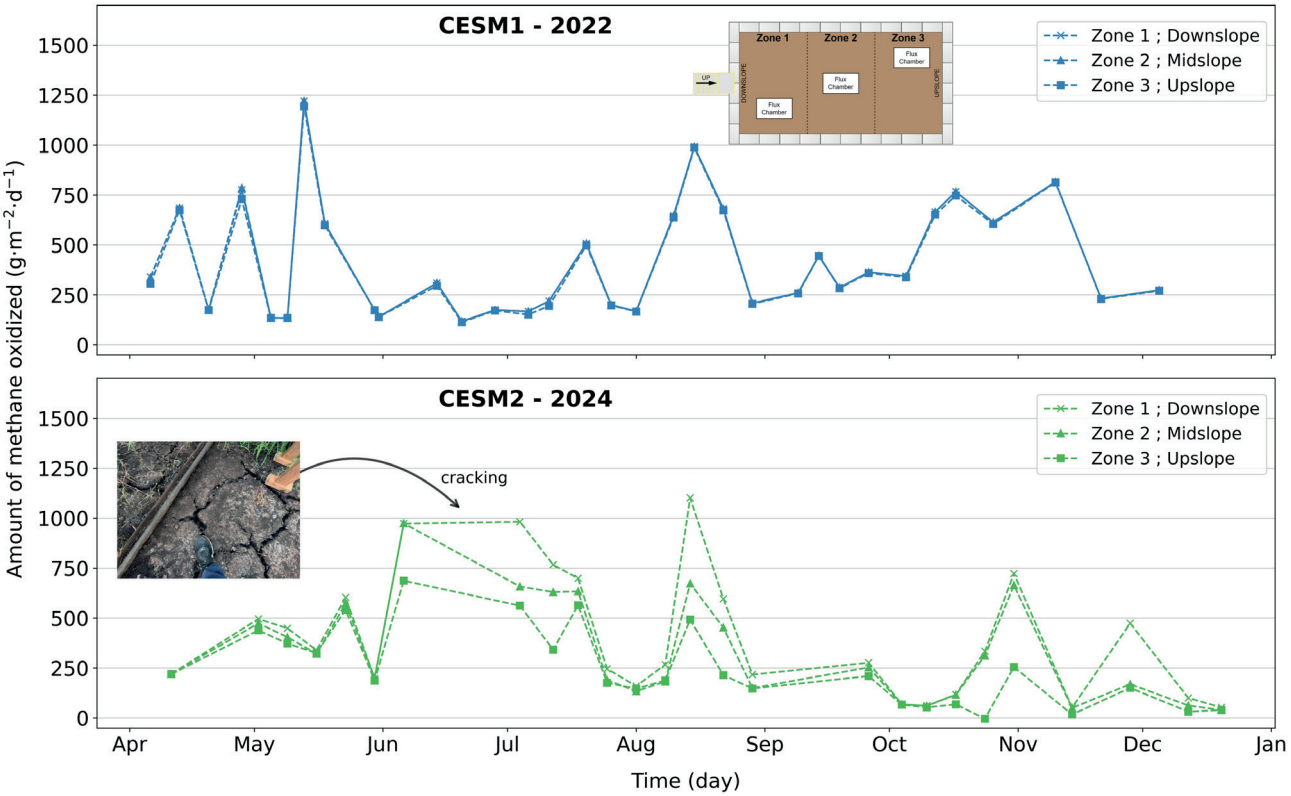

FIGURE 3: Temporal evolution of the amount of methane oxidised in the three biofilter zones for CESM1 (2022) and CESM2 (2024). CESM1 exhibits relatively uniform behavior among zones, whereas CESM2 shows pronounced spatial variability, particularly during summer months, with reduced performance in upslope zones associated with cracking and preferential flow.

between the two biofilters, as well as between zones where applicable. Statistical significance was established at $p < 0.05$.

All statistical analyses were conducted using Python (version 3.8.10).

3. RESULTS AND DISCUSSION

This section presents a comparative analysis of methane oxidation performance between the two project phases, CESM1 and CESM2. Although the systems were commissioned in different years (2021 for CESM1 and 2023 for CESM2), their initial operation began at similar times of the year (October). To minimize the influence of harsh winter conditions and exclude the initial stabilization period typical of newly commissioned experimental plots, the analysis focuses on the period from April to December. This time frame, spanning from early spring (snowmelt period) to the first weeks of winter, allows for the assessment of biofilter performance under relatively comparable meteorological conditions.

3.1 Amount of methane oxidized

Figure 3 illustrates the evolution of the amount of methane oxidized in the CESM1 (2022) and CESM2 (2024) biofilters, with data considered for each zone over time. We observe that both CESM1 and CESM2 exhibit variability in the amount of CH_4 oxidized over the monitored months. Additionally, a lower variation among zones is noted for CESM1. This observation is further supported by the descriptive statistical analysis (Table 1).

For CESM1, the amount of methane oxidized ranged from 113.1 to 1220.3 $g.m^{-2}.day^{-1}$, with median values of 297.5, 297.6, and 289.7 $g.m^{-2}.day^{-1}$ for zones 1, 2, and 3, respectively. For CESM2, the amount of methane oxidized ranged from 3.9 to 1101.4 $g.m^{-2}.day^{-1}$, with median values of 333.6, 252.9, and 187.8 $g.m^{-2}.day^{-1}$ for zones 1, 2, and 3, respectively. These results indicate that the fluctuation among zones was greater for CESM2 than for CESM1, as shown in Figure 3.

During the first quarter of the analysis period (April to June), CESM1 consistently oxidized slightly more methane than CESM2. Starting in June, a marked increase in methane oxidation was observed in CESM2, particularly in Zone 1 (downslope), reaching values close to 1000 $g.m^{-2}.day^{-1}$. However, this trend was accompanied by divergence among zones, especially from July onward, indicating an imbalance in gas distribution and/or spatial variability in microbial oxidative activity. Although gravel improves structural stability and drainage, its limited moisture retention capacity and absence of readily assimilable organic carbon may promote more localized microbial activity, which becomes strongly dependent on zones with more favorable moisture conditions and substrate availability (Huber-Humer et al., 2008).

The greater performance disparity among CESM2 zones, compared to CESM1, appears to be associated with microenvironmental modifications induced by the experi-

TABLE 1: Statistical data for CESM1 and CESM2 comparison.

Biofilter	Parameters	CH_4 loading	Efficiency	CH_4 oxidized - Z1	CH_4 oxidized – Z2	CH_4 oxidized – Z3
CESM 1	Mean	422.3	94.9	421.9	422.1	413.6
	Minimum	117.5	78.3	117.5	117.5	113.1
	Maximum	1223.1	99.9	1219.9	1220.3	1193.0
	Median	297.7	97.9	51.1	297.6	289.7
	Standar deviation	290.1	6.2	289.4	289.8	284.5
CESM 2	Mean	425.9	80.2	413.8	337.6	251.0
	Minimum	51.6	52.4	51.7	39.2	3.9
	Maximum	1240.5	100	1101.4	973.9	686.8
	Median	327.7	80.4	333.6	252.9	187.8
	Standar deviation	335.8	13.8	317.1	259.4	199.4
p-value		0.79	0.000011*	0.68	0.17	0.024*

*Values marked with * indicate statistically significant differences ($p < 0.05$) according to the Mann-Whitney test*

mental configuration. The installation of the shelter enclosure, which was required to enable continuous monitoring of methane oxidation, may have altered the thermal and hydric regimes within the biofilter. During the summer 2024 period, the shelter is expected to have enhanced internal heat accumulation. Combined with the lack of direct precipitation, these conditions led to accelerated desiccation of the MOL, causing a substantial decrease in its moisture content. Gómez-Borraz et al. (2025) showed that elevated temperatures in methane biofilters can shift microbial metabolism from anabolism toward catabolism due to thermal stress, ultimately impairing oxidation performance.

Taken together, these results reveal a clear trade-off between oxidation efficiency and total methane throughput. CESM1 consistently achieved higher and more stable oxidation efficiency, indicating robust performance of the open configuration and compost–woodchip MOL under a wide range of conditions. In contrast, CESM2 oxidised a larger total mass of methane, primarily because it was operated under substantially higher methane loadings during extended periods, despite exhibiting lower and more variable efficiency. From a design perspective, this highlights that systems optimized for stability and efficiency may differ from those intended to treat high methane fluxes. Enclosed configurations such as CESM2 can increase total abatement potential when higher loads are unavoidable, but require careful control of boundary conditions to prevent efficiency losses associated with drying, cracking, and preferential gas pathways.

Although the STEM material appeared adequately moist at the time of placement, progressive drying led to the development of surface fissures, predominantly in the midslope and upslope zones (zones 2 and 3). The formation of cracks facilitated preferential flow paths, thereby reducing methane residence time and limiting effective contact between the methane and the biologically active oxidation zone (Röwer et al. 2011; Gebert et al. 2022).

To mitigate these effects, we implemented corrective measures, including weekly manual irrigation applied at the surface of the biofilter and localized rehabilitation through excavation and compaction of the affected areas. These interventions led to an increase in methane oxidation from November 2024 onward in CESM2, suggesting a partial recovery of system performance following the restoration of moisture conditions and structural integrity.

Furthermore, the spatial variability in performance observed across CESM2 zones cannot be attributed to oxygen limitation, as both biofilters were supplied with a gas stream containing oxygen. This observation effectively excludes oxygen availability as a controlling factor and highlights the dominant influence of the thermal, hydric, and structural properties of the oxidation medium on methane oxidation performance under the investigated conditions.

Part of the variability observed in Figure 3 can be attributed to fluctuations in methane loading. As shown in Figure 5 (section 3.3.), methane loading influences oxidation efficiency, particularly in CESM2, which exhibits greater fluctuation across different loading ranges. This suggests that part of the apparent variation is not solely due to intrinsic system performance but is also driven by variations in inlet methane flux.

Despite the constraints, CESM2 oxidized a greater mass of methane during the summer of 2024, not due to higher efficiency, but rather because of its substantially greater methane loading (≈750 vs. 250 $g.m^{-2}.day^{-1}$). Consequently, although oxidation efficiency was lower, the total volume treated remained substantial. However, a statistically significant difference in overall oxidation efficiency was observed between CESM1 and CESM2 ($p < 0.05$), as shown in Table 2, with CESM1 showing higher performance; the oxidation efficiency itself is specifically addressed in Section 3.3. In addition, the amount of methane oxidized in Zone 3 was significantly higher in CESM1 compared to CESM2 ($p < 0.05$), indicating a spatially localized effect. This behavior appears to be associated with crack development in CESM2, particularly near Zone 3, highlighting the importance of structural integrity for maintaining biofilter performance.

To address the observed issues, targeted interventions were carried out between August and November 2024. These included manual excavation and compaction of deeply fissured areas, mainly in Zone 3, and surface till-

ing (≈30 cm depth) of the MOL across the entire biofilter. These adjustments led to a notable, albeit transient, increase in methane oxidation observed in November 2024, suggesting a partial restoration of uniform biogas distribution. Consequently, results from CESM2 should be interpreted with caution, as shelter induced disturbances may have disproportionately affected its performance, and do not necessarily reflect intrinsic material limitations under typical field conditions.

The dataset presented in Figure S2 (Supplementary Material II) comprises water content, temperature, and the amount of methane oxidized data for the CESM2 system from October to December 2024. Due to technical and operational constraints, sensor data were not available for other months. Nevertheless, this period provides important insights into the hydric and thermal conditions governing methane oxidation during the transition from autumn to early winter.

From October to November 2024, water content in Zone 1 remained relatively high, with values around 0.32 m^3/m^3, while Zone 2 exhibited lower moisture levels, ranging from 0.20 to 0.10 m^3/m^3, confirming the spatial heterogeneity previously identified in CESM2 (Figure S1). After November 2024, a pronounced decrease in water content was observed in both zones, with Zone 1 decreasing to 0.10–0.04 m^3/m^3 and Zone 2 reaching values as low as 0.02 m^3/m^3. Rather than being directly associated with summer conditions, this drying trend reflects the combined effects of reduced precipitation input and continued influence of the shelter enclosure, which limits natural rewetting of the MOL.

In CESM1, water content profiles were monitored over a longer period, from April to December 2022, as also reported by Almeida et al. (2024). During this period, moisture content ranged from 0.35 m^3/m^3 to 0.80 m^3/m^3 (Figure S3, Supplementary material III), indicating consistently higher water availability compared to CESM2. Similarly to CESM2, higher moisture levels were observed in Zone 1, suggesting a recurring spatial pattern within the system, probably influenced by slope and preferential water accumulation.

The temperature profile for CESM2 (Figure S4) in October 2024 revealed pronounced spatial variability among zones, with higher temperatures observed in Zone 2 (54.5°C) compared to Zone 1 (31.2-43.8°C). This indicates the presence of localized thermal hotspots within the system, probably associated with differences in gas flux distribution and microbial activity, as well as the influence of the shelter enclosure on heat retention.

At 1 m depth, corresponding to the base of the MOL (CESM2), temperatures in November 2024 were 35.3°C, 30.6°C, and 23.7°C for zones 1, 2, and 3, respectively (Figure S5, Table S5, Supplementary material V). In December 2024, a consistent decrease in temperature was observed across all zones, reaching 27.6°C, 24.3°C, and 19.6°C. This cooling trend is consistent with the transition toward colder seasonal conditions and suggests a progressive reduction in thermal energy within the system.

The elevated temperature observed in Zone 2 in October 2024 may have contributed to suboptimal conditions for methane oxidation. Although moderate increases in temperature can enhance microbial activity, excessively high temperatures, such as those exceeding 50°C, may induce thermal stress in methanotrophic communities, shifting metabolism and potentially reducing oxidation efficiency (Gómez-Borraz et al. 2025).

Considering the period from October to December 2022 in CESM1, corresponding to the same seasonal window analyzed for CESM2 in 2024, the average temperature did not vary significantly among zones, remaining within a relatively narrow range between 50°C and 62°C (see Figure S6, Supplementary material VI). This thermal uniformity contrasts with the pronounced spatial variability observed in CESM2.

The more homogeneous temperature distribution in CESM1 suggests a more stable internal environment, possibly associated with the absence of the shelter enclosure and the resulting natural exchange of heat and moisture with the atmosphere.

Furthermore, the combination of high temperatures and the previously observed moisture conditions may have intensified spatial heterogeneity in methane oxidation. While Zone 2 exhibited higher temperatures, its lower moisture content compared to Zone 1 suggests that the balance between thermal conditions, water availability, and gas diffusivity plays a critical role in controlling system performance. Nevertheless, beyond these site-specific effects, both systems exhibited similar temporal trends consistent with seasonal patterns, suggesting that ambient temperature may have influenced methane oxidation dynamics.

A decline in efficiency was observed during the summer (2022, 2024) for both biofilters, followed by a temporary peak in August and a subsequent drop in early September. An additional decrease in performance occurred at the beginning of winter, pointing to a shared seasonal response across both systems. This pattern indicates an influence of temperature and moisture on system performance. Elevated summer temperatures promoted drying, affecting methanotrophic activity, gas diffusion, and structural integrity. In CESM2, high temperatures caused surface cracking (especially in Zone 3) as discussed before. A similar trend was observed in CESM1, where temperatures reached 43-52°C in August 2022 (Almeida et al., 2024), followed by a decline below 40°C. Although continuous data in August 2024 were unavailable for CESM2, the consistency between systems suggests that seasonal heating and drying drove the observed dynamics, with the shelter amplifying these effects.

3.2 Methane oxidation capacity with batch tests

As part of the CESM2 phase, we conducted batch tests in August 2024, shortly after the marked decline in performance observed in July 2024, to assess the impact of disturbances, fissuring, on the methane oxidation capacity of the MOL. Three field samples were collected, one from each zone, and compared to a reference material from CESM1, also sampled by zone. This CESM1 material, collected at the end of the project (2022), was stored in an airtight 18 L container and kept active through weekly injections of 500 mL of pure methane.

Figure 4 illustrates the performance differences across the two biofilter phases, revealing a marked decrease in microbial activity in the CESM2 samples.

While the CESM1 compost fully oxidized the methane within 10 hours, with an initial oxidation rate of 1.55% $CH_4 \cdot h^{-1}$, CESM2 samples displayed a comparable rate during the first two to three hours (1.29% $CH_4.h^{-1}$), followed by a significant slowdown (0.27% $CH_4.h^{-1}$) reflecting microbial stress or partial dormancy due to dry and fissured field conditions in CESM2.

These findings reinforce the hypothesis that the shelter enclosure modified boundary conditions and impaired biofilter performance. The poorest-performing batch (Zone 3, upslope) aligned with the most fissured field zone, indicating that physical disruption adversely affected microbial activity. This is consistent with Figure 3, which shows lower oxidation in Zone 3 during the summer. In contrast, CESM1 exhibited high and stable oxidative capacity across all zones, in both batch and field conditions.

Considering this, adapting the operational strategy of the biofilter to the specific constraints imposed by the enclosed configuration appears necessary, particularly to mitigate heat-related effects such as cracking. Enhancing moisture content and ensuring a more homogeneous gas distribution within CESM2 are expected to improve the overall oxidation rate while simultaneously reducing the pronounced heterogeneity among zones. In parallel, an acclimatization protocol was launched in December 2024 to reestablish microbial activity, with ongoing monitoring to evaluate long-term recovery trends.

3.3 Effect of load on the methane oxidation efficiency

Figure 5 shows the distribution of oxidation efficiencies across methane loading rates for both phases. CESM1 exhibited predominantly high efficiencies (>95% in 33 instances), sustained across a wide range of methane loadings, including elevated values (>900 $g.m^{-2}.day^{-1}$). This pattern reflects the biofilter's ability to maintain high efficiency despite substantial variations in methane input.

Several studies have reported that the landfill gas loading rate can control the diffusion of atmospheric oxygen into biofilter media, thereby limiting microbial methane oxidation (Dever et al. 2011). However, in the present study, oxygen availability was not a limiting factor, as the gas supplied to the biofilters contained approximately 18.5% O_2. In the study by Farrokhzadeh et al. (2017), methane oxidation efficiencies ranging from 80 to 95% were achieved even under high methane loadings (370 - 1112 $g.m^{-2}.day^{-1}$). This sustained performance was attributed to the adopted aeration strategy, which effectively prevented oxygen limitation and ensured adequate O_2 availability for microbial oxidation.

By contrast, CESM2 displayed greater variability, with 16 of 26 measurements falling below 80%, highlighting the biosystem's operational instability. Notably, the six lowest-performing measurements (<70%) were all recorded under low methane loadings (0-150 $g.m^{-2}.day^{-1}$), suggesting reduced efficiency of the system even under moderate operating conditions. Only four CESM2 measurements exceeded 95% efficiency, all at lower loads (<650 $g.m^{-2}.day^{-1}$), comparing to CESM1, suggesting limited high-performance range. However, when compared with other studies, such as Falk et al. (2025), methane loadings of approximately 650 $g.m^{-2}.day^{-1}$ were among the highest values investigated. This comparison indicates that, although CESM2 exhibited lower performance than CESM1, the biofilter under CESM2 conditions still demonstrated generally good methane oxidation performance.

Some physical and chemical properties of the materials used in the MOL of both systems could, at first moment, explain the observed differences in performance. For instance, CESM2 exhibited a significantly lower total porosity (48%) compared to CESM1 (69%), which could theoretically limit gas diffusion through the medium. However, air permeability and air-filled porosity were comparable,

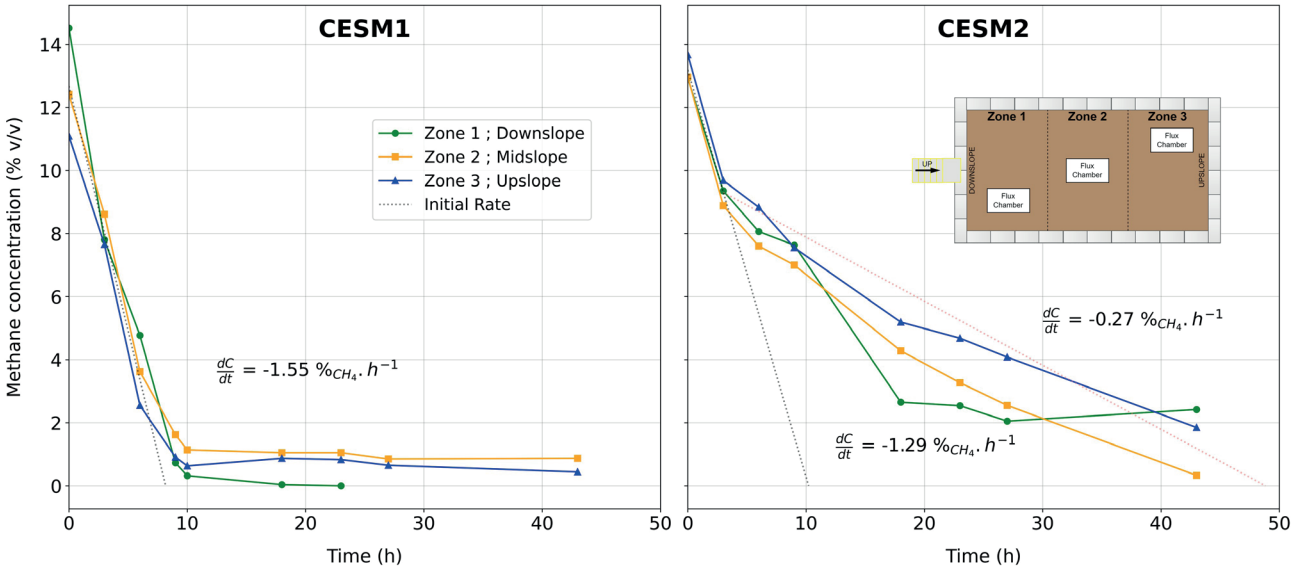

FIGURE 4: Methane consumption kinetics by zone for CESM1 and CESM2.

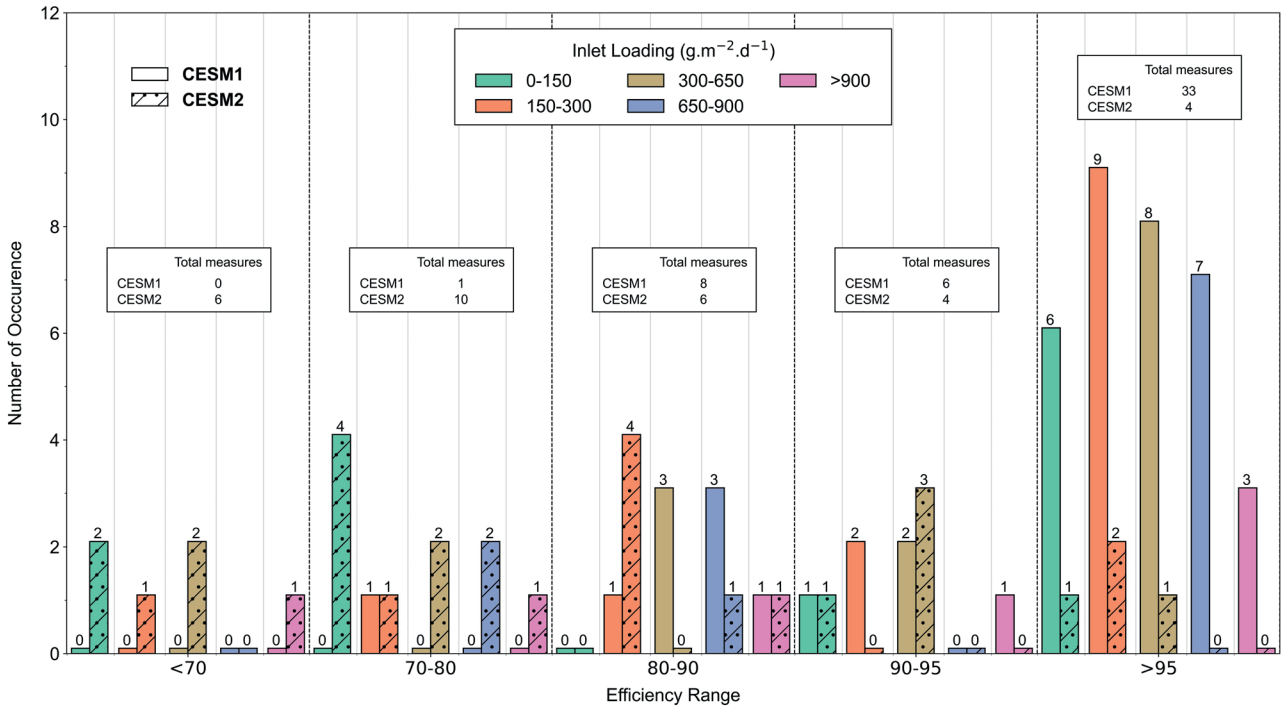

FIGURE 5: Relationship between methane loading rate and oxidation efficiency for CESM1 and CESM2. CESM1 maintains consistently high efficiencies across a wide loading range, while CESM2 displays greater variability and reduced efficiency at both low and high loadings, indicating higher sensitivity to operational and boundary-condition effects.

suggesting that gas transfer limitations were not primarily responsible for the observed performance differences. Furthermore, the air-filled porosity values of 31% for CESM1 and 28% for CESM2 (Table 2) are well above the minimum threshold of 14% identified by Gebert et al. (2011) as suitable for effective methane oxidation in biofilter systems.

In terms of organic matter content, the compost used in CESM1 (44%) was markedly richer than that of CESM2 (6.7 %), potentially supporting a denser and more active methanotrophic community. This may help explain CESM1's field performance. Nonetheless, the kinetic profile of CESM2 still reflects strong intrinsic potential, suggesting that its lower performance was not solely due to biological limitations, but also influenced by physical factors such as reduced porosity or even boundary conditions like the presence of a shelter enclosure. These findings emphasize the importance of both material composition and structural properties in determining biofilter effectiveness.

Although CESM1 benefitted from a prior acclimatization phase, the evidence points toward the shelter enclosure in CESM2 as a major limiting factor. Localized heat accumulation and surface fissuring, particularly in Zone 3, disrupted gas distribution within the MOL. In several cases, surface methane concentrations near fissures were equivalent to inlet values, confirming the formation of preferential pathways that bypassed the MOL and compromised the biofilter's overall efficiency.

The contrasted behavior of CESM1 and CESM2 highlights several practical implications for the design and operation of field-scale methane oxidation biofilters. In CESM1, the clogging observed at the MOL–GDL interface illustrates the limitations of incorporating fine sand filter layers beneath high-organic-matter compost media. Degradation and migration of organic components can lead to pore occlusion and cementation, ultimately restricting gas transfer and reducing long-term reliability. These observations underline the importance of ensuring hydraulic and textural compatibility between adjacent layers, favoring materials with comparable permeability to minimize the risk of persistent clogging.

The performance of CESM2 further emphasizes the need to carefully balance structural stability and moisture retention in the selection of structuring agents for structured engineered media. Although gravel enhanced mechanical stability and drainage, reduced water-holding capacity contributed to desiccation, spatial heterogeneity, and reduced microbial robustness under field conditions. These effects were amplified by the presence of the shelter enclosure, which modified thermal and hydric boundary conditions by limiting natural precipitation inputs and promoting heat accumulation. In enclosed or semi-enclosed configurations, such boundary-condition effects should therefore be explicitly addressed through design measures aimed at moderating temperature and maintaining adequate moisture levels, such as controlled ventilation, shading, or supplemental irrigation.

Finally, the development of surface cracking and preferential gas pathways in CESM2 demonstrates the critical role of surface integrity in maintaining effective methane oxidation. Cracking reduced methane residence time and promoted localized bypass, particularly in upslope zones, leading to reduced apparent efficiency despite high micro-

TABLE 2: Characteristics of MOL materials.

Properties	Standard	CESM1	CESM2
Grain size distribution Gravel (5 mm < D < 112 mm) Sand (0.08 mm < D < 5 mm) Silt (D < 0.08 mm)	14688-2 (ISO, 2017)	9.0% 88.0% 3.0%	77.9% 20.2% 1.9%
Specific gravity (ρ_s)	D854-23 (ASTM, 2023)	2.03 g.cm^{-3}	2.50 g.cm^{-3}
Field dry density (ρ_d)	D7263-21(ASTM, 2021)	0.63 g.cm^{-3}	1.30 g.cm^{-3}
Total Porosity (n)	-	69%	48%
Volumetric water content (θ)	D2216-19 (ASTM, 2019)	38 m³/m³	20 m³/m³
Air-filled porosity (θ_a)	-	31%	28%
Organic matter (%w/w)	D2974-20 (ASTM, 2020)	44%	6.7%
Dry Air permeability (m.s^{-1})	D6539 – 13 (ASTM_International, 2013)	8.4 x 10^{-5}	7.0 x 10^{-5}
Maximum oxidation capacity ($V_{máx}$)	-	2 383 g.m^{-3}.day^{-1}	1 624 g.m^{-3}.day^{-1}
Km	-	12 g.m^{-3}	23.4 g.m^{-3}

bial potential. Routine surface inspection and timely corrective interventions, including rewetting, recompaction, or shallow tilling, appear essential to sustain uniform gas distribution and stable performance over time. Collectively, these observations show that biofilter performance is governed not only by intrinsic material properties but also by construction details and boundary conditions, which must be jointly considered in practical design and operation.

4. CONCLUSIONS

This study highlighted key differences and shared patterns between the CESM1 and CESM2 biofilters. Seasonal trends confirmed the role of ambient conditions, while lab tests showed that CESM1's STEM had higher methane oxidation capacity. Both substrates, however, maintained a good oxidation potential. In the field, CESM1 delivered stable performance, whereas CESM2 showed higher variability and reduced efficiency.

This variability was primarily linked to the CESM2 shelter enclosure, which altered the thermal and hydraulic conditions within the system. These changes led to overheating, MOL cracking (especially in Zone 3), and gas bypass. Batch tests confirmed microbial activity loss, leading to remedial actions and a reacclimatization protocol.

Corrective measures began in fall 2024, with microbial recovery underway over winter. These findings show that while enclosures facilitate continuous monitoring, they can disrupt gas and moisture dynamics. Such effects must be addressed in the design of enclosed biosystems to ensure stable and efficient methane oxidation.

Based on these findings, the following practical recommendations can be drawn:

- Avoid full enclosure without appropriate moisture and temperature control systems.
- Monitor and mitigate drying and cracking, particularly in upslope zones.
- Ensure a balance between structural stability and organic matter content in STEM design to maintain both permeability and microbial activity.

Future work will focus on developing enclosure designs that allow continuous monitoring while minimizing adverse effects such as drying, overheating, and gas flow heterogeneity.

ACKNOWLEDGEMENTS

The authors would like to thank the BiomethoxUS research group from l'Université de Sherbrooke. They also thank the employees of the Complexe Environmental de Saint-Michel (CESM). The corresponding author and Professor Alexandre Cabral were funded by the Natural Sciences and Engineering Research Council of Canada (NSERC: ALLRP 586235-23 and ALLRP 577053).

REFERENCES

Abichou, T., Powelson, D., Chanton, J., Escoriaza, S., & Stern, J. (2006). Characterization of Methane Flux and Oxidation at a Solid Waste Landfill. Journal of Environmental Engineering, 132(2), 220–228. https://doi.org/10.1061/(ASCE)0733-9372(2006)132:2(220)

Ahoughalandari, B., Cabral, A. R., & Leroueil, S. (2018). Elements of design of passive methane oxidation biosystems: fundamental and practical considerations about compaction and hydraulic characteristics on biogas migration. Geotechnical and Geological Engineering, 36(4), 2593-2609. https://doi.org/10.1007/s10706-018-0485-z

Almeida, J. L., Dumouchel, J., Santos, J. J. N., Dulac, Y., Cabral, A. R., & Héroux, M. (2024). Construction, monitoring, and efficiency of a biofilter treating a high flow, lean, landfill gas. Waste Management, 190, 455–464. https://doi.org/10.1016/j.wasman.2024.10.007

ASTM. (2019). D2216-19: Standard Test Methods for Laboratory Determination of Water (Moisture) Content of Soil and Rock by Mass (Nos D2216-19). https://www.astm.org/d2216-19.html

ASTM. (2021). D7263-21: Standard Test Methods for Laboratory Determination of Density and Unit Weight of Soil Specimens (No.D7263-21). https://www.astm.org/d7263-21.html

ASTM. (2023). D854-23: Standard Test Methods for Specific Gravity of Soil Solids by the Water Displacement Method (Nos D854-23). https://www.astm.org/d0854-23.html

ASTM D2974-14. (2020). Standard Test Methods for Moisture, Ash, and Organic Matter of Peat and Other Organic Soils (No. ASTM D2974-14). ASTM International. https://doi.org/10.1520/D2974-14

ASTM_International. (2013). ASTM D6539-13 Standard Test Method for Measurement of the Permeability of Unsaturated Porous Materials by Flowing Air. https://doi.org/10.1520/D6539

City of Montréal. (2020). Montréal Climate Plan: Objective carbon-neutral by 2050. Ville de Montréal. https://montreal.ca/en/articles/montreal-climate-plan-objective-carbon-neutral-2050-7613

Dever, S. A., Swarbrick, G. E., & Stuetz, R. M. (2011). Passive drainage and biofiltration of landfill gas: Results of Australian field trial. Waste Management, 31(5), 1029-1048. https://doi.org/10.1016/j.wasman.2010.10.026

Duan, Z., Scheutz, C., & Kjeldsen, P. (2022). Mitigation of methane emissions from three Danish landfills using different biocover systems. Waste Management, 149, 156–167. https://doi.org/10.1016/j.wasman.2022.05.022

Dulac, Y., & Cabral, A. (2025). Determination of the Water Occlusion Point of Structured Engineered Media Based on Air Permeability Testing [Paper submitted for publication].

Dulac, Y., Nelson, B. R., Zytner, R. G., & Cabral, A. R. (2024). Validation of a Methane Oxidation Biosystem Design Methodology Using Numerical Modeling. Frontiers in Environmental Science, 12, 1397134. https://doi.org/10.3389/fenvs.2024.1397134

ECCC. (2022). Climate Plan—Reducing methane emissions [Government]. Environment and Climate Change Canada. https://www.canada.ca/en/services/environment/weather/climatechange/climate-plan/reducing-methane-emissions.html

Falk, J. M., Kjeldsen, P., Fredenslund, A. M., Buck, C., & Scheutz, C. (2025). Design and establishment of a biofilter for treatment of manure methane emissions. Waste Management, 206, 115087. https://doi.org/10.1016/j.wasman.2025.115087

Farrokhzadeh, H., Hettiaratchi, J. P. A., Jayasinghe, P., & Kumar, S. (2017). Aerated biofilters with multiple-level air injection configurations to enhance biological treatment of methane emissions. Bioresource Technology, 239, 219–225. https://doi.org/10.1016/j.biortech.2017.05.009

Franzidis, J.-P., Héroux, M., Nastev, M., & Guy, C. (2008). Lateral migration and offsite surface emission of landfill gas at City of Montreal landfill site. Waste Management & Research, 26(2), 121–131. https://doi.org/10.1177/0734242X07085752

Gebert, J., Huber-Humer, M., & Cabral, A. R. (2022). Design of Microbial Methane Oxidation Systems for Landfills. Frontiers in Environmental Science, 10, 907562. https://doi.org/10.3389/fenvs.2022.907562

Gebert, J., Röwer, I.U., Scharff, H., Roncato, C.D.L., Cabral, A.R., 2011. Can Soil Gas Profiles Be Used to Assess Microbial CH4 Oxidation in Landfill Covers? Waste Management 31, 987–994. https://doi.org/10.1016/j.wasman.2010.10.008

Gomez-Borraz, T. L., Torres-Arévalo, Y. V., Cuetero-Martínez, Y., González-Sánchez, A., & Noyola, A. (2025). Assessment of temperature dynamics during methane oxidation in a pilot scale compost biofilter. Bioresource Technology, 419, 132097. https://doi.org/10.1016/j.biortech.2025.132097

He, R., Ma, R.-C., Yao, X.-Z., & Wei, X.-M. (2017). Response of methanotrophic activity to extracellular polymeric substance production and its influencing factors. Waste Management, 69, 289–297. https://doi.org/10.1016/j.wasman.2017.08.019

Huber-Humer, M., Gebert, J., & Hilger, H. (2008). Biotic Systems to Mitigate Landfill Methane Emissions. Waste Management & Research, 26(1), 33–46. https://doi.org/10.1177/0734242X07087977

ISO. (2017). 14688-2: Geotechnical investigation and testing—Identification and classification of soil (Nos 14688–2). https://www.iso.org/standard/66346.html

La, H., Hettiaratchi, J. P. A., Achari, G., Verbeke, T. J., & Dunfield, P. F. (2018). Biofiltration of methane using hybrid mixtures of biochar, lava rock and compost. Environmental Pollution, 241, 45–54. https://doi.org/10.1016/j.envpol.2018.05.039

Lagos, D. A., Héroux, M., Gosselin, R., & Cabral, A. R. (2017). Optimization of a landfill gas collection shutdown based on an adapted first-order decay model. Waste Management, 63, 238–245. https://doi.org/10.1016/j.wasman.2016.08.012

QED Environmental Systems Inc., 2017. SEM 5000 Surface Emissions Monitor. URL https://www.qedenv.com/products/portable-methane-detector-sem5000/ (accessed 23.03.26).

Röwer, I. U., Geck, C., Gebert, J., & Pfeiffer, E. M. (2011). Spatial variability of soil gas concentration and methane oxidation capacity in landfill covers. Waste management, 31(5), 926-934. https://doi.org/10.1016/j.wasman.2010.09.013

Scheutz, C., Duan, Z., Møller, J., & Kjeldsen, P. (2023). Environmental assessment of landfill gas mitigation using biocover and gas collection with energy utilisation at aging landfills. Waste Management, 165, 40-50. https://doi.org/10.1016/j.wasman.2023.04.014

Souza, J. C. M., Neto, M. D. O., Dulac, Y., Santos, J. J. N., Galli, F., & Cabral, A. R. (2025). Continuous monitoring approach for estimating methane oxidation efficiency in biosystems. In Proceedings of Sardinia 2025 – 19th International Symposium on Waste Management and Sustainable Landfilling. CISA Publisher.